Spray and evaporation characteristics of ethanol and gasoline direct injection in non-evaporating, transition and flash-boiling conditions

Yuhan Huang [a,b], Sheng Huang [a], Ronghua Huang [a,*], Guang Hong [b]

Affiliations:

[a] State Key Laboratory of Coal Combustion, Huazhong University of Science and Technology, Wuhan, China

[b] School of Electrical, Mechanical and Mechatronic Systems, University of Technology Sydney, Sydney, Australia

Corresponding author:

Ronghua Huang, PhD

Postal address: State Key Laboratory of Coal Combustion, Huazhong University of Science and Technology, 1037 Luoyu Road, Wuhan, China, 430074

Email: rhhuang@hust.edu.cn

Telephone: +86-27-87541518

KEYWORDS

Direct injection; Non-evaporating; Flash-boiling; Excess temperature; Spray transition process.

ABSTRACT

Ethanol direct injection plus gasoline port injection (EDI+GPI) represents a more efficient and flexible way to utilize ethanol fuel in spark ignition engines. To exploit the potentials of EDI, the mixture formation characteristics need to be investigated. In this study, the spray and evaporation characteristics of ethanol and gasoline fuels injected from a multi-hole injector were investigated by high speed Shadowgraphy imaging technique in a constant volume chamber. The experiments covered a wide range of fuel temperature from 275 K (non-evaporating) to 400 K (flash-boiling) which corresponded to cold start and running conditions in an engine. The spray transition process from normal- evaporating to flash-boiling was investigated in

greater details than the existed studies. Results showed that ethanol and gasoline sprays demonstrated the same patterns in non-evaporating conditions. The sprays could be considered as non-evaporating when vapour pressure was lower than 30 kPa. Ethanol evaporated more slowly than gasoline did in low temperature environment, but they reached the similar evaporation rates when temperature was higher than 375 K. This suggested that EDI should only be applied in high temperature engine environment. For both ethanol and gasoline sprays, when the excess temperature was smaller than 4 K, the sprays behaved the same as the subcooled sprays did. The sprays collapsed when the excess temperature was 9 K. Flash-boiling did not occur until the excess temperature reached 14 K. The fuel temperature changed not only the spray evaporation modes but also the breakup mechanisms.

1. INTRODUCTION

Gasoline direct injection (GDI) has several advantages over port fuel injection, including improved fuel economy and transient response, more precise air-fuel ratio control, extended EGR tolerance limit, selective emissions advantages and enhanced potential for system optimization [1-3]. On the other hand, ethanol is a widely used alternative fuel to address the issue of sustainability. Compared with gasoline fuel, ethanol has greater enthalpy of vaporization, larger octane number, higher flame speed and smaller stoichiometric air/fuel ratio [4-6]. Recently, ethanol direct injection (EDI) has attracted much attention due to its great potential in taking the advantages of ethanol fuel to increase the compression ratio and thermal efficiency [7-10]. The engine knock propensity could be reduced by the higher octane number of ethanol fuel, and supplemented by the strong cooling effect enhanced by EDI. These advantages make it possible to increase the compression ratio and use turbocharging (engine downsizing technologies) for spark ignition (SI) engines while avoiding the knock issue, and consequently increase the thermal efficiency.

To exploit the potentials of EDI, the spray and mixture formation characteristics should be investigated as they are the key factors that influence the combustion and emissions of the engine. Experimental results showed that the NOx emission decreased, and CO and HC emissions increased with EDI injection in a gasoline port injection engine [7]. The NOx emission was decreased due to the cooling effect enhanced by EDI and CO

and HC emissions were increased due to poor mixing, local over-cooling and fuel impingement at high load conditions [11, 12]. However opposite experimental results were reported in [13]. NOx emission increased and CO and HC emissions decreased when EDI was applied. Furthermore, both HC and NOx emissions were reduced by EDI as reported in [8]. The above different results might be caused by the evaporation process of EDI spray in different engine conditions in different investigations.

The fuel evaporation process strongly affects the consequent mixture formation, combustion and emission processes. This is because the droplets must vaporize before they can burn [14, 15]. However, little work has been done in this field. A better vaporization of ethanol fuel was used to explain the experimental results of decreased spray tip penetration and increased spray angle with the increase of ethanol/gasoline fraction [16]. Some reported a slower vaporization of ethanol spray than gasoline's because of the light components in gasoline fuel [17]. It was found that ethanol had a faster vaporization rate due to its higher vapour pressure in high temperature conditions in experiments [18]. Numerical studies showed that the evaporation rate of ethanol direct injection was lower than that of gasoline in naturally aspirated SI engines [4, 19]. However the simulated evaporation rate of ethanol was as high as that of gasoline in a turbocharged engine [20]. It was found that the fuel temperature played an important role in the evaporation process of ethanol spray. Ethanol evaporated more slowly than gasoline did in low temperature conditions, but faster when temperature was higher than 375 K [4].

The fuel temperature can change in a wide range from non-evaporating (cold start in winter) to flash-boiling sprays in real engine conditions. The effect of fuel temperature on gasoline spray injected by swirl-type injectors was investigated [21-24]. It was found that the spray collapsed with faster evaporation rate, longer penetration and smaller droplet size when the temperature was above the saturation temperature. Recently, the multi-hole injectors have attracted more attention for direct injection SI engines because of their advantages in stability of spray pattern and flexibility of spray plume targeting [25]. However the majority of work published to date on multi-hole injectors concerns diesel nozzles [26]. Aleiferis et al. conducted extensive experiments on the multi-hole injector spray behaviors of various fuels and ambient conditions [26-30]. The studies were focused on the spray shape transformation of flash- boiling sprays (or spray collapse: transition from

multi-jet spray to single-jet spray) either by increasing the fuel temperature or decreasing the ambient pressure. Zeng et al. investigated the transition process from non-flash boiling to flare flash boiling sprays using alcohol fuels [31]. It was reported that the spray flash boiling occurred at Pa/Ps=1 (ambient-to-saturation pressure ratio) and spray collapsed at Pa/Ps=0.3. However, recent study for ethanol spray from a multi-hole injector found that the spray flash boiling did not occur as soon as the liquid temperature was higher than the boiling point (Pa/Ps=1) [32].

The adequate performance of direct injection systems is the key factor to achieve the benefits of GDI and EDI. Since ethanol fuel has lower stoichiometric air/fuel ratio and heating value, more mass of ethanol should be injected into the cylinder in order to maintain the same output power and equivalence ratio. More injected fuel results in larger spray momentum and longer spray tip penetration, which may lead to fuel impingement on cylinder and piston walls. Besides, gasoline and ethanol sprays would show different breakup regimes (Bag Breakup, Stripping Breakup, or Catastrophic Breakup) or vaporisation patterns (flash or non-flash boiling sprays) due to their different physical properties [31, 33]. The spray flash-boiling may occur in engine conditions which would destroy the designed spray directions and mixture distributions [26, 31]. Therefore, investigating the spray and evaporation characteristics is of great importance for extending the use of ethanol fuel.

In this study, the effect of fuel temperature on the ethanol and gasoline spray characteristics from a multi-hole injector has been studied in a constant volume chamber as part of investigation of a novel fuel system, ethanol direct injection plus gasoline port injection (EDI+GPI) [7]. The fuel temperature varied from 275 K (non-evaporating) to 400 K (flash-boiling) which corresponded to cold-start and running conditions that the injector may have in real engines. The effect of fuel temperature on evaporation rates of ethanol and gasoline was investigated. The flash-boiling was observed by increasing fuel temperature in atmospheric pressure. Particularly, the spray transition process from normal-evaporating to flash-boiling was investigated in greater details than the existed studies.

2. EXPERIMENTAL SECTION

2.1. Injector

The injector used in this study was a 6-hole nozzle which was used in the experimental investigations of an EDI+GPI research engine [7]. The nozzle diameter measured using a microscope was 110 μm, as shown in Fig. 1(a). The emanated spray bends to the direction of the injector solenoid valve, as illustrated in Fig. 1(b). The six plumes are distributed in three groups. The first group contains only one plume whose axis is the same as that of the injector. The second group contains three plumes and the bend angle is 17° to the injector axis. The third group contains two plumes and the bend angle is 34°.

2.2. Test Fuels

The ethanol fuel investigated in this study was the absolute ethyl alcohol with a purity of 99.9%. The gasoline fuel tested was a commercial unleaded gasoline with an octane number of 97. Fig. 2 shows the fuel properties of ethanol and gasoline over the temperature range investigated in the present study. These thermo-chemistry properties were calculated using correlations from the Prausnitz' and Yaws' Handbooks and experimental data [34-36]. Specifically, the boiling point of ethanol fuel in atmospheric pressure is 351 K. Although gasoline fuel consists of organic compounds ranging from C2 to C14 and it does not have a uniform boiling point, a nominal boiling point for gasoline can be drawn based on the vapour pressure-temperature profile. In atmospheric pressure, the nominal boiling point of gasoline is 341 K (Fig. 2(d)). The temperatures 351 K and 341 K are the points where ethanol and gasoline sprays may present different patterns respectively.

2.3. Experimental apparatus

Fig. 3 is a schematic of the experimental apparatus including the constant volume chamber, the fuel injection system, the Schlieren/Shadowgraphy optical system and the vacuum system. The chamber has a shape of a cube with edge length of 136 mm. The diameter of the quartz window is 130 mm. Silicon heating sheets were adhered to the outer surfaces of the chamber body. The chamber was covered by insulating layer. A digital temperature controller was used to regulate the temperature with the feedback from a platinum resistance

thermometer plugged into the chamber near the injector. Therefore the fuel temperature (injector temperature) and ambient gas temperature were the same as the chamber body temperature when the heating process reached a balance. The injector was mounted horizontally with its axis perpendicular to the light pathway. The light source was a GB/T14094-1993 tungsten halogen lamp. The voltage for the lamp was kept at 100 V to supply the same light source for each measurement. Two nitrogen cylinders were used to pressurize and control the injection pressure and ambient pressure respectively. The injection pulse width 2.0 ms was generated by a single-chip computer. Meanwhile, the pulse was sent to trigger the MotionPro Y4S1 high speed CCD camera simultaneously. Shadowgraphy and Schlieren techniques are two of the most effective techniques used to visualize the time-resolved non-homogeneous transparent flow fields, such as the evaporating sprays and reacting spray flames. The only difference in these two methods is that a knife edge (item 16 in Fig. 3) is used in front of the camera in Schlieren technique but not in Shadowgraphy technique. Schlieren technique uses the knife edge to enhance the contrast but may lose some information [37, 38]. The knife edge was not used and only the Shadowgraphy measurements were performed because the gas turbulence was weak and light attenuation through the air was low enough to highlight the spray area for the quiescent ambient conditions in the present study.

2.4. Experimental conditions

The fuel injection pressure of 6 MPa was achieved using compressed nitrogen. 6 MPa was the direct injection pressure of the ethanol fuel applied in the experiments on the EDI+GPI research engine [7]. The ambient pressure was kept at 1 bar which represented the cylinder pressure during early EDI injection [4]. The tested fuel temperature varied from 275 K (non-evaporating spray) to 400 K (flash-boiling spray) with an increment of 25 K. However the temperature increment was reduced to 5 K during the spray transition process from normal-evaporating to flash-boiling. The injection pulse width was 2 ms. The speed of the imaging was 20000 fps @ 608 × 288 pixels. The spatial resolution of the images was 0.203 mm/pixel. Each spray temperature condition was repeated for five times. To measure the fuel mass per injection pulse, the fuel injected of 300 consecutive sprays was collected and measured on a mass balance with an accuracy of 1 mg (1 mg over about 3000 mg).

147 The measured fuel mass per injection was 10.84 mg and 9.02 mg @ 6 MPa × 2 ms for EDI and GDI
148 respectively. The uncertainty of the fuel mass measurement was within 2% (standard deviation of five
149 measurements).

150 2.5. Image Processing

151 The captured images were 8-bit grey scale images. The images were processed using a Matlab code. Fig. 4
152 demonstrates the procedure of the spray image processing code. Firstly, the spray image (Fig. 4(b)) was
153 background corrected using a frame prior to the fuel injection (Fig. 4(a)). This step eliminated the uncertainty of
154 the back lighting and background noise caused by the gas flows in the chamber. Then, a threshold of 5% was
155 used to convert the background corrected image (Fig. 4(c)) to a binary image (Fig 4(d)). The sensitivity of the
156 threshold value has been tested in a previous study [32]. Finally the boundary of spray area (Fig. 4(e)) can be
157 determined based on the binary image (Fig. 4 (d)). The macroscopic spray characteristics were calculated based
158 on the spray boundary. As shown in Fig. 4(f), the spray tip penetration was defined as the longest distance that
159 the spray travelled. The spray projected area was the area within the spray boundary. The spray angle was
160 defined according to the SAE J2715 Standard [39]. Four points have been located on the spray boundary: two
161 near points have a horizontal distance of 5 mm to the injector tip, and the distance for the two farther points is
162 15 mm. These four points were used to define two lines on each side of the spray boundary. The angle of the
163 two lines was defined as the spray angle. The averaged image pixel intensity values were calculated based on
164 the images without the background noise (background corrected image Fig. 4(c)). The spray tip penetration,
165 angle, projected area and averaged image pixel intensity reported in the following sections were the averaged
166 values of five repeated experiments. Error bars (±1 standard deviation) were used to show the statistical
167 uncertainty of each data point in Figs. 7 and 8.

168 3. RESULTS AND DISCUSSION

169 3.1. Macroscopic characteristics of non-evaporating, normal-evaporating and flash-boiling sprays

170 Fig. 5 shows the ethanol spray patterns at fuel temperature varying from 275 K to 400 K with an increment of
171 25 K. As shown in Fig. 5, the three ethanol plumes are narrow and the plume boundary is smooth when the

fuel temperature is 275 K (non-evaporating spray). When the temperature is increased from 275 K to 325 K, the plumes become wider and a swirl forms at the tip of the third spray plume, indicating a stronger interaction between the droplets and ambient gas. However, at temperatures of 275, 300 and 325 K, the spray plumes are narrow and can be clearly identified. When the fuel temperature is further increased from 325 K to 350 K which is close to ethanol's boiling point 351 K, the plumes become wider and difficult to be distinguished at 0.5 ms after the start of injection (ASOI), but can be identified after 1.0 ms ASOI. At 350 K, the plume-plume and plume-air interactions are more significant. The first and third plume groups move towards the middle one. At the same time, a big swirl is formed at the tip of the third plume. The spray droplets lose their penetration momentum more quickly, resulting in a shorter penetration. Significant changes occur to the ethanol spray when the temperature is higher than the boiling point (351 K). Fig. 5 shows that, at temperatures lower than 350 K, the dark color in the ethanol spray tip at 0.10 ms ASOI shows clear edge of the plume. However, at 375 and 400 K, the droplet explosion process can be observed at the injector tip when the first droplets are emanated into the air at 0.1 ms ASOI, as indicated by the arrows. A small dark spray area is surrounded by a light area. The light area is again surrounded by a dark area. This is because the droplet is superheated when it is injected into the low pressure ambient gas. Vapour bubbles may form inside the droplet and burst the droplet into smaller ones, resulting in the dark and light areas observed. The explosion process makes the plume-air and plume-plume interactions much stronger. The plume boundaries of flash-boiling sprays become more turbulent and the three plumes integrate into a single one and become totally unrecognizable.

Fig. 6 shows gasoline spray patterns at different fuel temperatures. Compared with ethanol spray, the effect of fuel temperature on gasoline spray is more significant. At 275 K, the gasoline spray patterns are the same to that of ethanol spray whose plumes are narrow and have smooth boundaries. However, when the fuel temperature is increased from 275 K to 325 K, the gasoline spray behaves like the ethanol spray at 350 K. A big swirl is formed at the tip of the third gasoline spray plume, which reduces the spray tip penetration. Meanwhile, the two side plumes move towards the middle one. Finally when the temperature reaches 350 K, the gasoline spray collapses while the ethanol spray can still maintain its shape at the same temperature, indicating that gasoline

spray structure is more sensitive to the fuel temperature and has a lower spray collapse temperature than ethanol does. This is because typical gasoline contains about 35–40% C5 or lower hydrocarbon chains, and similar levels of C6–C8 [26, 31]. The boiling point of n-hexane (C6H14) is 342 K [34]. This indicates that about 50% of the gasoline compositions have lower boiling points than ethanol does. In fact, the nominal boiling point of gasoline is 341 K in atmospheric pressure. The light components in gasoline evaporate readily and have significant effect on the spray characteristics. The droplet explosion effect is more obvious in gasoline sprays than that in ethanol sprays when fuel temperatures are 375 K and 400 K, as shown by the bigger bright area (indicated by arrows) in the gasoline spray tip at 0.1 ms ASOI in Fig. 6.

Fig. 7 shows the effect of fuel temperature on spray tip penetration, spray angle and spray projected area of ethanol and gasoline fuels. In real fuel injection systems, no two injections can be identical and shot-to-shot variability is inevitable due to the high turbulence of high pressure liquid jets [40]. The error bars (standard deviation) represents the uncertainty of the measurements. As the temperature increases, the uncertainty becomes larger, showing by the bigger error bars of spray projected area and angle in Fig. 7. This is due to the increased plume-air and plume-plume interactions (increased turbulence level) in high temperature conditions. Nevertheless, the effect of fuel temperature on the macroscopic spray characteristics is still clearly shown by Fig. 7. As shown in Figs. 7(a) and 7(b), ethanol and gasoline have very similar penetrations in low temperature environments (<325K for ethanol and <300K for gasoline). Same conclusions were reported in previous studies with different fuels or injectors. Ref. [26] investigated the spray development of iso-octane, n-pentane, gasoline, ethanol and n-butanol with a multi-hole injector. Ref. [41] investigated spray characteristics of gasoline-ethanol blends with a multi-hole port fuel injector. Ref. [42] investigated the sprays of bioethanol and bioethanol blended gasoline with a high pressure swirl injector. Ref. [17] investigated the spray characterization of gasoline (E0), E50 and ethanol (E100) fuels with multi-hole gasoline direct injectors. Supporting the conclusions in previous studies, a same conclusion was drawn that ethanol and gasoline fuels showed similar/identical spray penetrations in low temperature conditions. However the penetration decreases in higher temperatures (325-350 K for ethanol and 300-350 K for gasoline) because of the increased evaporation rates.

When further increasing the temperature into flash-boiling region (375-400 K), the penetration lengths are shorter than that of 350K spray's in early spray stages (<2.0 ms ASOI for ethanol and <1.0 ms ASOI for gasoline), but longer after that. This is because the collapsed spray plumes focus all their momentum into a single direction and thus enhance the penetration. The longer penetrations of flash-boiling sprays were also observed in [17, 31, 43]. Figs. 7(c) and 7(d) show projected areas of ethanol and gasoline sprays. Generally, gasoline has a smaller projected area than ethanol does at the same temperature because of gasoline's faster evaporation rate than ethanol's. The spray projected areas increase slightly with the increase of fuel temperature within 275-325 K for ethanol and 275-300 K for gasoline, but decrease when the temperature is further increased because of the significantly increased spray evaporation. This will be further discussed in section 3.2. The spray areas decrease more significantly in the flash-boiling region. When the temperature reaches 400 K, the projected areas of ethanol at 7.0 ms ASOI and gasoline at 5.5 ms ASOI reduce to a value of approximately zero which means the liquid fuel is fully evaporated. Regarding the spray angle, as shown in Figs. 7(e) and 7(f), the effect of fuel temperature on spray angle is not obvious when the temperature is lower than 350 K. However when the fuel temperature is higher than 350 K, the spray angles become much smaller because of the spray collapse. Moreover, the spray angles show decreasing trend at 375 K but increasing trend at 400 K for both ethanol and gasoline sprays.

3.2. Evaporation characteristics and implications for engine emissions

The effect of the fuel temperature on the spray evaporation rate is visible in Figs. 5 and 6 with the images at 8 ms ASOI. The time 8 ms is about the evaporation time (9.5 ms) allowed for early EDI timing started at 300° BTDC, ignition timing of 15° BTDC and engine speed of 5000 rpm in the engine experiments [7]. It can be seen that the color of the spray area become brighter with the increase of the fuel temperature, which indicates a faster evaporation rate. To quantify it, the averaged pixel intensity value of the spray area is shown in Fig. 8. A larger value means higher concentration of the spray droplets and thus lower evaporation rate. As shown in Fig. 8, the pixel intensity of 275 K ethanol spray at 8 ms ASOI is 10.6. It only reduces slightly to 10.5 at 300 K and 10.2 at 325 K. Further increase of fuel temperature results in significant decrease of the pixel intensity.

Therefore, the evaporation of ethanol fuel only increases slightly when the fuel temperature is increased from 275 K to 325 K, but significantly from 325 K to 400 K. On the other hand, gasoline shows faster evaporation than ethanol does over the temperature range investigated. Moreover, the temperature, over which the spray evaporates quickly, of gasoline (300 K) is lower than that of ethanol (325 K). The evaporation rate is greatly increased when flash-boiling occurs. As shown in Fig. 8, the pixel intensity value of ethanol spray decreases from 8.5 at 350 K to 5.0 at 375 K and further to 2.1 at 400 K. However, gasoline spray only decreases from 5.8 at 350 K to 3.8 at 375 K and to 1.9 at 400 K. This indicates that the evaporation rate of ethanol is increased more than gasoline does in high temperature conditions. This is because the heavy components in gasoline fuel evaporate slowly. By 400 K, ethanol spray reaches a similar evaporation completeness (2.1) as that of gasoline spray (1.9).

Saturation vapour pressure is an important factor to indicate the liquid's volatility and the driving force for the fuel evaporation. Table 1 lists the vapour pressures of ethanol and gasoline fuels at the temperatures investigated. It will be used to assist the discussion of results in Fig. 8. Fig. 8 shows that the evaporation rates of ethanol at temperatures lower than 325 K and gasoline at temperatures lower than 300 K are low and similar. This indicates that the spray can be considered as non-evaporating when the vapour pressure is lower than 30 kPa (325 K for ethanol and 300 K for gasoline). In the normal-evaporating region (325-350 K), gasoline spray evaporates much faster than ethanol spray does, but they reach the same evaporation rate when the temperature is higher than 375 K. The tendency revealed in this study is consistent with the results in the previous numerical study which reported that the ethanol fuel evaporated more slowly than gasoline did in low temperature environment (<375 K), but faster in high temperature environment (>375 K) [4]. Experiments in a constant volume chamber showed that ethanol evaporated more slowly than gasoline did in a low temperature environment of 333 K [17]. Experiments in an optical engine operated in partial load and 20 or 80 ℃ coolant temperature found that fuels with high ethanol proportions evaporated more slowly than that with low ethanol proportions did [44]. However experiments in high temperature environment (500 K) found that ethanol evaporated faster than gasoline did [45]. Same result was reported in [18] with gasoline and ethanol fuels at

272 temperature of 450 K.

273 As the evaporation process affects the consequent combustion and emission generation significantly, the slow
274 evaporation rate of ethanol fuel in low temperature environment must be taken into account in developing the
275 EDI+GPI engine. Experimental results on an EDI+GPI engine showed that the CO and HC emissions increased
276 when EDI was applied [7]. The low compression ratio 9.8 and high engine speed 3500-5000 rpm indicate low
277 temperature environment and short time for fuel evaporation. However experiments on a same dual-injection
278 fuel system reported the decrease in CO and HC emissions with EDI, in which the engine had a higher
279 compression ratio of 11.5 and lower engine speed of 1500 rpm [8, 13]. The injection timing was 300° BTDC in
280 [7] and 280° BTDC in [8, 13]. The unfavourable conditions (short time and low temperature) for EDI
281 evaporation in [7] would have caused the increased CO and HC emissions. Numerical studies showed that the
282 evaporation rate of EDI was lower than that of gasoline in naturally aspirated spark ignition engines [4, 19].
283 However the simulated evaporation rate of ethanol was as high as that of gasoline in a turbocharged engine
284 [20]. These results suggest that EDI should only be applied in high temperature environments, such as high
285 compression ratio, full-load or turbocharged engines, to improve the fuel evaporation and mixture preparation
286 processes and consequently avoid the increased CO and HC emissions.

287 3.3. Spray Transition Process

288 Fig. 9 shows the transition process from normal-evaporating spray to flash-boiling spray of ethanol and gasoline
289 fuels. The spray excess temperature ΔT is used to quantify the superheat degrees. Fig. 9 shows that flash-boiling
290 does not occur as soon as the fuel temperature is higher than the boiling temperature. There is no significant
291 difference in the patterns between the sprays at ΔT=4 K and that at subcooled temperatures (350 K for ethanol
292 and 340 K for gasoline). Compared with subcooled sprays, the swirl at the spray tip becomes larger and the first
293 and third plumes move more closely to the middle one when the spray is slightly superheated (ΔT=4 K).
294 However the three plumes can still be recognised at 1.0 ms ASOI for ΔT=4 K sprays. When ΔT reaches 9 K,
295 the sprays collapse completely for both ethanol and gasoline fuels. The three plumes join together and become
296 unidentifiable. Therefore, the transition temperatures of spray collapse at atmospheric pressure are 360 K

297 and 350 K for ethanol and gasoline fuels respectively. The spray droplet explosion does not occur until ΔT
298 reaches 14 K, as indicated by the arrows at 0.1 ms ASOI. When ΔTs are 14 K and 19 K, spray clouds in much
299 lighter colour start to appear at the spray tip. This is because the spray droplets start to evaporate and boil
300 internally. The droplet explosion accelerates the breakup and evaporation greatly. Moreover, for multi-
301 component fuels such as gasoline, the light components may flash boil before the fuel reaches the nominal
302 boiling point. As shown in the images in Fig. 9(b) at 0.5 ms ASOI, some bright bubbles can be seen in the first
303 plume of gasoline sprays, but not in ethanol sprays.

304 The results shown in Fig. 9 are consistent with that of experiments for superheated water droplets [46]. As
305 reported in [46], when ΔT was below 5 K, the evaporation was on the surface. The droplets started to boil
306 internally when the ΔT was between 5 K and 18 K, but they did not flash and disintegrate until ΔT was above
307 18 K. Zeng et al. investigated the spray transformation process of n-hexane, methanol and ethanol fuels [31].
308 They used the ambient-to-saturation pressure ratio (Pa/Ps) to quantify the spray superheat degrees and
309 concluded that flash-boiling occurred at Pa/Ps=1.0 and plume collapse occurred at Pa/Ps=0.3. However,
310 experiments in this study found that neither flash-boiling nor plume collapse occurred as soon as the fuel
311 temperature was higher than the boiling point (Pa/Ps=1). Instead, the spray maintained its structure when the
312 spray was slightly superheated (ΔT < 4 K) and flash boiled when spray was further superheated (ΔT > 14 K).
313 Recent study in an optical engine showed that spray did not collapse when the Pa/Ps was 0.85, but collapsed
314 when Pa/Ps reached 0.63 [47]. The spray flash boiled before it collapsed in Zeng's experiments was mainly
315 because the injector had a relatively big angle of 60° between the plume axis, while the spray angle of the
316 injector used in the present study was only 17°. This implies that the temperature of spray collapse is dependent
317 on the spray angle of the injector, so that injectors with larger spray angles have higher spray collapse
318 temperatures.

319 As the fuel temperature increases from the normal-evaporating region to the flash-boiling region, the droplet
320 breakup mechanism changes as well. Based on the breakup mechanism which depends on the Weber number

($We = \rho u^2 d/\sigma$), droplet breakup can be classified into bag breakup (12<*We*<80), stripping breakup (80<*We*<350) and catastrophic breakup (*We*>350) [48]. Where ρ is the density of the gas, u is the relative velocity of the droplet, d is the undisturbed droplet radius, σ is the surface tension of the droplet. Fig. 10 shows the Weber numbers of primary break-up droplets of ethanol and gasoline sprays at the nozzle exit varying with fuel temperature. The Weber number is an important indicator for the choosing of breakup models in spray simulation [49]. The primary droplets are very close to the nozzle exit, which are only tens of nozzle hole diameters away from the injector tip (intact core length) [33, 50]. Therefore the *u* is assumed be the jet velocity, which is 100 m/s ($u = C_D\sqrt{2\Delta P/\rho}$). The *d* is determined based on the blob injection concept, which assumed the primary droplet to be the similar size of the nozzle diameter [51-53]. As shown in Fig. 10, when temperature is lower than 390 K, the ethanol Weber number is less than 80 which is in the regime of bag breakup. The ethanol breakup regime becomes catastrophic breakup when the temperature is higher than 485 K. On the other hand, the effect of fuel temperature on gasoline spray is less significant. Below 370 K, the gasoline spray is in the regime of bag breakup. The gasoline spray remains in the stripping breakup regime even when the temperature reaches 500 K. Higher Weber number means shorter breakup time and faster breakup rate, thus leads to smaller droplet size and higher evaporation rate.

4. CONCLUSIONS

The high speed Shadowgraphy imaging technique was used to investigate the spray and evaporation characteristics of ethanol and gasoline fuels injected from a multi-hole injector as part of investigation of the ethanol direct injection plus gasoline port injection (EDI+GPI) engine, which is a new fuelling and combustion module. Experiments were conducted in a constant volume chamber with fuel temperature varied from 275 K (non-evaporating) to 400 K (flash-boiling). Particularly the spray transition process from normal-evaporating to flash-boiling was investigated. The major conclusions of this study are as follows:

(1) Ethanol and gasoline sprays showed the same patterns in non-evaporating conditions. As fuel temperature increased, it had greater effect on gasoline spray structure than on ethanol's, indicated by lower spray collapse temperature of gasoline than that of ethanol. The effect of fuel temperature on macroscopic characteristics was insignificant for non-flash boiling sprays, but significant for flash-boiling sprays whose spray angles and projected areas became much smaller and the spray tip penetrations were slightly longer.

(2) Ethanol evaporated more slowly than gasoline did in low temperature environment (< 375 K), but they reached a similar evaporation rate when the fuel temperature was higher than 375 K. The sprays could be considered as non-evaporating when the vapour pressure was smaller than 30 kPa, demonstrated by the low evaporation rates at temperature lower than 325 K for ethanol and 300 K for gasoline. The evaporation rates increased significantly when temperatures were further increased. The low evaporation rate of ethanol fuel in low temperature environment implied that EDI should only be applied in high temperature engine environment.

(3) For both ethanol and gasoline sprays, flash-boiling (droplet explosion) did not occur when the fuel temperature was higher than the boiling point until the excess temperature reached 14 K. When excess temperature was smaller than 4 K, the sprays behaved the same as subcooled sprays did. The sprays collapsed at excess temperature of 9 K. The spray collapse temperature was dependent on the spray angle of the injector, where injectors with larger spray angles had higher transition temperatures.

(4) Not only the spray evaporation modes but also the breakup mechanisms changed with the fuel temperature. The ethanol spray went through all the three breakup mechanisms within the temperature range from 275 K to 500 K, while gasoline spray only went through the bag breakup and stripping breakup regimes.

ACKNOWLEDGMENT

The scholarship provided by the China Scholarship Council (CSC) is gratefully appreciated. The authors

would like to express their great appreciation to Mr. Yinjie MA, Dr. Peng DENG and the workshop at the Huazhong University of Science and Technology (HUST) in China for their technical assistance and support.

ABBREVIATIONS

ASOI=after the start of injection; *EDI*=ethanol direct injection; *GDI*=gasoline direct injection; *SI*=spark ignition; *EDI+GPI*=ethanol direct injection plus gasoline port injection; *Pa/Ps*=ambient-to-saturation pressure ratio; ΔT=spray excess temperature; *We*=droplet Weber number; ρ=density; u=velocity; σ=surface tension; d=diameter.

REFERENCES

[1] F. Zhao, M.C. Lai, D.L. Harrington. Automotive spark-ignited direct-injection gasoline engines. Progress in Energy and Combustion Science 1999; 25: 437-562.

[2] W. Qin, D.L.S. Hung, M. Xu. Investigation of the temporal evolution and spatial variation of in-cylinder engine fuel spray characteristics. Energy Conversion and Management 2015; 98: 430-439.

[3] M. Costa, U. Sorge, L. Allocca. Increasing energy efficiency of a gasoline direct injection engine through optimal synchronization of single or double injection strategies. Energy Conversion and Management 2012; 60: 77-86.

[4] Y. Huang, G. Hong, X. Cheng, R. Huang. Investigation to Charge Cooling Effect of Evaporation of Ethanol Fuel Directly Injected in a Gasoline Port Injection Engine. SAE paper 2013-01-2610; 2013.

[5] A. Boretti. Towards 40% efficiency with BMEP exceeding 30bar in directly injected, turbocharged, spark ignition ethanol engines. Energy Conversion and Management 2012; 57: 154-166.

[6] C. Liang, C. Ji, B. Gao, X. Liu, Y. Zhu. Investigation on the performance of a spark-ignited ethanol engine with DME enrichment. Energy Conversion and Management 2012; 58: 19-25.

[7] Y. Zhuang, G. Hong. Primary Investigation to Leveraging Effect of Using Ethanol Fuel on Reducing Gasoline Fuel Consumption. Fuel 2013; 105: 425-431.

[8] X. Wu, R. Daniel, G. Tian, H. Xu, Z. Huang, D. Richardson. Dual-injection: The flexible, bi-fuel concept

391 for spark-ignition engines fuelled with various gasoline and biofuel blends. Applied Energy 2011; 88: 2305-
392 2314.
393 [9] R.A. Stein, C.J. House, T.G. Leone. Optimal Use of E85 in a Turbocharged Direct Injection Engine. SAE
394 Int. J. Fuels Lubr. 2009; 2: 670-682.
395 [10] D.R. Cohn, L. Bromberg, J. Heywood. Fuel Management System for Variable Ethanol Octane
396 Enhancement of Gasoline Engines. US Patent 2010175659; 15 July, 2010.
397 [11] Y. Huang, G. Hong, R. Huang. Numerical investigation to the dual-fuel spray combustion process in an
398 ethanol direct injection plus gasoline port injection (EDI+GPI) engine. Energy Conversion and Management
399 2015; 92: 275-286.
400 [12] Y. Huang, G. Hong, R. Huang. Investigation to charge cooling effect and combustion characteristics of
401 ethanol direct injection in a gasoline port injection engine. Applied Energy 2015; 160: 244-254.
402 [13] R. Daniel, C. Wang, H. Xu, G. Tian, D. Richardson. Dual-Injection as a Knock Mitigation Strategy Using
403 Pure Ethanol and Methanol. SAE Int. J. Fuels Lubr. 2012; 5: 772-784.
404 [14] W.W. Pulkrabek. Engineering Fundamentals of the Internal Combustion Engine. Prentice-Hall, Inc.; 1997.
405 [15] P. Jenny, D. Roekaerts, N. Beishuizen. Modeling of turbulent dilute spray combustion. Progress in Energy
406 and Combustion Science 2012; 38: 846-887.
407 [16] J. Gao, D. Jiang, Z. Huang. Spray Properties of Alternative Fuels: A Comparative Analysis of Ethanol–
408 Gasoline Blends and Gasoline. Fuel 2007; 86: 1645-1650.
409 [17] A. Matsumoto, W.R. Moore, M.-C. Lai, Y. Zheng, M. Foster, X.-B. Xie, D. Yen, K. Confer, E. Hopkins.
410 Spray Characterization of Ethanol Gasoline Blends and Comparison to a CFD Model for a Gasoline Direct
411 Injector. SAE Int. J. Engines 2010; 3: 402-425.
412 [18] H. Oh, C. Bae, K. Min. Spray and Combustion Characteristics of Ethanol Blended Gasoline in a Spray
413 Guided DISI Engine under Lean Stratified Operation. SAE Int. J. Engines 2010; 3: 213-222.
414 [19] S. Srivastava, H. Schock, F. Jaberi, D.L.S. Hung. Numerical Simulation of a Direct-Injection Spark-
415 Ignition Engine with Different Fuels. SAE paper 2009-01-0325; 2009.

[20] P.K. Kasseris, Knock Limits in Spark Ignited Direct Injected Engines Using Gasoline/Ethanol Blends, in: Dept. of Mechanical Engineering, Massachusetts Institute of Technology, PhD Thesis, Cambridge, 2011.

[21] L. Araneo, A. Coghe, G. Brunello, R. Dondé. Effects of Fuel Temperature and Ambient Pressure on a GDI Swirled Injector Spray. SAE paper 2000-01-1901; 2000.

[22] K. Nakama, E. Murase, M. Imada, J. Kusaka, Y. Daisho. Effects of High Temperature Fuel on In-Cylinder Fuel Mixture Formation Process for Direct Injection Engine. SAE paper 2003-32-0003; 2003.

[23] E. Murase, K. Nakama, S. Toyoda, J. Kusaka, Y. Daisho. The Effects of Fuel Temperature on a Direct Injection Gasoline Spray in a Constant Volume Chamber. SAE paper 2003-01-1810; 2003.

[24] K. Kannaiyan, R. Sadr. Experimental investigation of spray characteristics of alternative aviation fuels. Energy Conversion and Management 2014; 88: 1060-1069.

[25] A. Matsumoto, Y. Zheng, X.-B. Xie, M.-C. Lai, W. Moore. Characterization of Multi-hole Spray and Mixing of Ethanol and Gasoline Fuels under DI Engine Conditions. SAE paper 2010-01-2151; 2010.

[26] P.G. Aleiferis, Z.R. van Romunde. An analysis of spray development with iso-octane, n-pentane, gasoline, ethanol and n-butanol from a multi-hole injector under hot fuel conditions. Fuel 2013; 105: 143-168.

[27] J. Serras-Pereira, P.G. Aleiferis, D. Richardson, S. Wallace. Characteristics of Ethanol, Butanol, Iso-Octane and Gasoline Sprays and Combustion from a Multi-Hole Injector in a DISI Engine. SAE Int. J. Fuels Lubr. 2008; 1: 893-909.

[28] Z. van Romunde, P.G. Aleiferis, R.F. Cracknell, H.L. Walmsley. Effect of Fuel Properties on Spray Development from a Multi-Hole DISI Engine Injector. SAE Paper 2007-01-4032; 2007.

[29] P.G. Aleiferis, J. Serras-Pereira, Z. van Romunde, J. Caine, M. Wirth. Mechanisms of spray formation and combustion from a multi-hole injector with E85 and gasoline. Combustion and Flame 2010; 157: 735-756.

[30] P.G. Aleiferis, J. Serras-Pereira, A. Augoye, T.J. Davies, R.F. Cracknell, D. Richardson. Effect of fuel temperature on in-nozzle cavitation and spray formation of liquid hydrocarbons and alcohols from a real-size optical injector for direct-injection spark-ignition engines. International Journal of Heat and Mass Transfer 2010; 53: 4588-4606.

441 [31] W. Zeng, M. Xu, G. Zhang, Y. Zhang, D.J. Cleary. Atomization and vaporization for flash-boiling multi-
442 hole sprays with alcohol fuels. Fuel 2012; 95: 287-297.
443 [32] Y. Huang, S. Huang, P. Deng, R. Huang, G. Hong. The Effect of Fuel Temperature on the Ethanol Direct
444 Injection Spray Characteristics of a Multi-hole Injector. SAE Int. J. Fuels Lubr. 2014; 7: 792-802.
445 [33] F.V. Bracco. Modeling of Engine Sprays. SAE paper 850394; 1985.
446 [34] C.L. Yaws. Yaws' Handbook of Thermodynamic and Physical Properties of Chemical Compounds.
447 Knovel; 2003.
448 [35] K. Kar, T. Last, C. Haywood, R. Raine. Measurement of Vapor Pressures and Enthalpies of Vaporization
449 of Gasoline and Ethanol Blends and Their Effects on Mixture Preparation in an SI Engine. SAE Int. J. Fuels
450 Lubr. 2008; 1: 132-144.
451 [36] B.E. Poling, J.M. Prausnitz, J.P. O'Connell. The Properties of Gases and Liquids (Fifth Edition).
452 McGRAW-HILL; 2001.
453 [37] J.V. Pastor, J.M. García, J.M. Pastor, L.D. Zapata. Evaporating Diesel Spray Visualization using a Double-
454 pass Shadowgraphy/Schlieren imaging. SAE paper 2007-24-0026; 2007.
455 [38] J.V. Pastor, R. Payri, J.M. Garcia-Oliver, F.J. Briceño. Schlieren Methodology for the Analysis of
456 Transient Diesel Flame Evolution. SAE Int. J. Engines 2013; 6: 1661-1676.
457 [39] Gasoline Fuel Injector Spray Measurement and Characterization. SAE standard J2715; 2007.
458 [40] J. Kostas, D. Honnery, J. Soria. Time resolved measurements of the initial stages of fuel spray penetration.
459 Fuel 2009; 88: 2225-2237.
460 [41] T.N.C. Anand, A. Madan Mohan, R.V. Ravikrishna. Spray characterization of gasoline-ethanol blends
461 from a multi-hole port fuel injector. Fuel 2012; 102: 613-623.
462 [42] S.H. Park, H.J. Kim, H.K. Suh, C.S. Lee. Atomization and spray characteristics of bioethanol and
463 bioethanol blended gasoline fuel injected through a direct injection gasoline injector. International Journal of
464 Heat and Fluid Flow 2009; 30: 1183-1192.
465 [43] B. Zhu, M. Xu, Y. Zhang, G. Zhang. Physical Properties of Gasoline-Alcohol Blends and Their Influences
466 on Spray Characteristics from a Low Pressure DI Injector. Proceedings of the 14th Asia Annual

Conference on Liquid Atomization and Spray Systems (ILASS-Asia); 2010.

[44] L. Chen, R. Stone, D. Richardson. A study of mixture preparation and PM emissions using a direct injection engine fuelled with stoichiometric gasoline/ethanol blends. Fuel 2012; 96: 120-130.

[45] M. Chato, S. Fukuda, K. Sato, T. Fujikawa, R. Chen, Z. Li, J. Tian, K. Nishida. Fuel Spray Evaporation and Mixture Formation Processes of Ethanol/Gasoline Blend Injected by Hole-Type Nozzle for DISI Engine. SAE Int. J. Engines 2012; 5: 1836-1846.

[46] Handbook of Atomization and Sprays: Theory and Applications. Springer; 2011.

[47] Q.N. Chan, Y. Bao, S. Kook. Effects of injection pressure on the structural transformation of flash-boiling sprays of gasoline and ethanol in a spark-ignition direct-injection (SIDI) engine. Fuel 2014; 130: 228-240.

[48] N. Zeoli, S. Gu. Numerical modelling of droplet break-up for gas atomisation. Computational Materials Science 2006; 38: 282-292.

[49] D. Jajcevic, R. Almbauer, S. Schmidt, K. Glinsner, M. Fitl. CFD Study of Spray Design for a GDI High Performance 2-Stroke Engine. SAE paper 2010-32-0014; 2010.

[50] M. Xie. Computational Combustion Theory of IC Engines (in Chinese). 2nd ed., Dalian, China: Dalian University of Technology Press; 2005.

[51] L. Postrioti, F. Mariani, M. Battistoni. Experimental and numerical momentum flux evaluation of high pressure Diesel spray. Fuel 2012; 98: 149-163.

[52] S. Jafarmadar. Three-dimensional modeling and exergy analysis in Combustion Chambers of an indirect injection diesel engine. Fuel 2013; 107: 439-447.

[53] X. Jiang, G.A. Siamas, K. Jagus, T.G. Karayiannis. Physical Modelling and Advanced Simulations of Gas–liquid Two-phase Jet Flows in Atomization and Sprays. Progress in Energy and Combustion Science 2010; 36: 131-167.

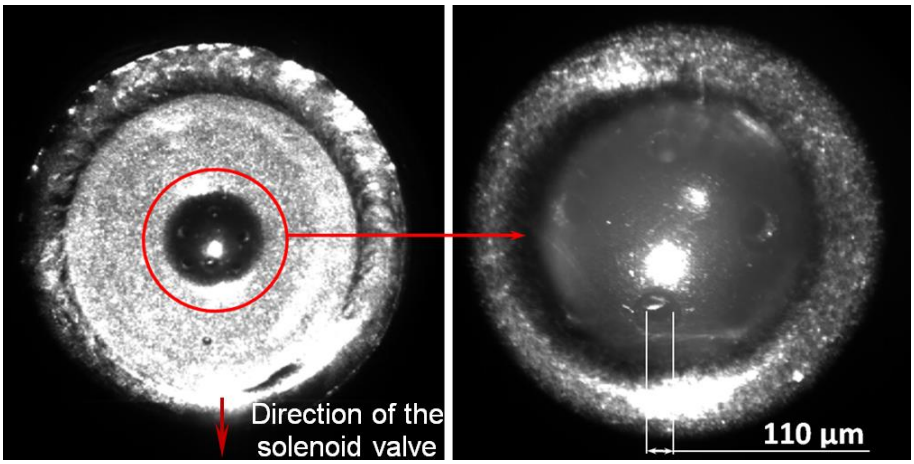

(a)

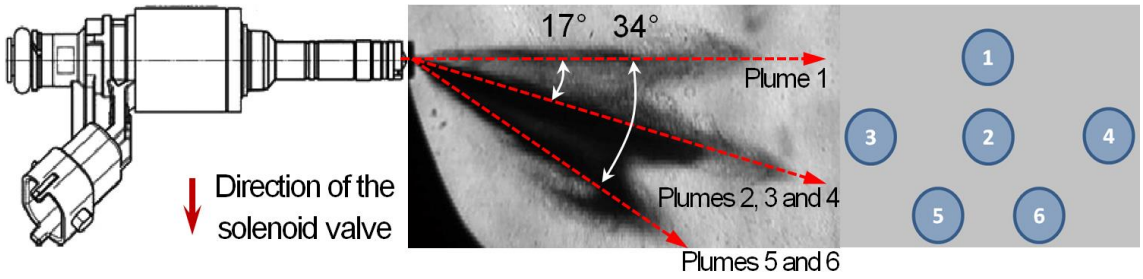

(b)

Fig. 1. Schematic of the injector: (a) distributions of the nozzle holes, (b) plume directions and footprints.

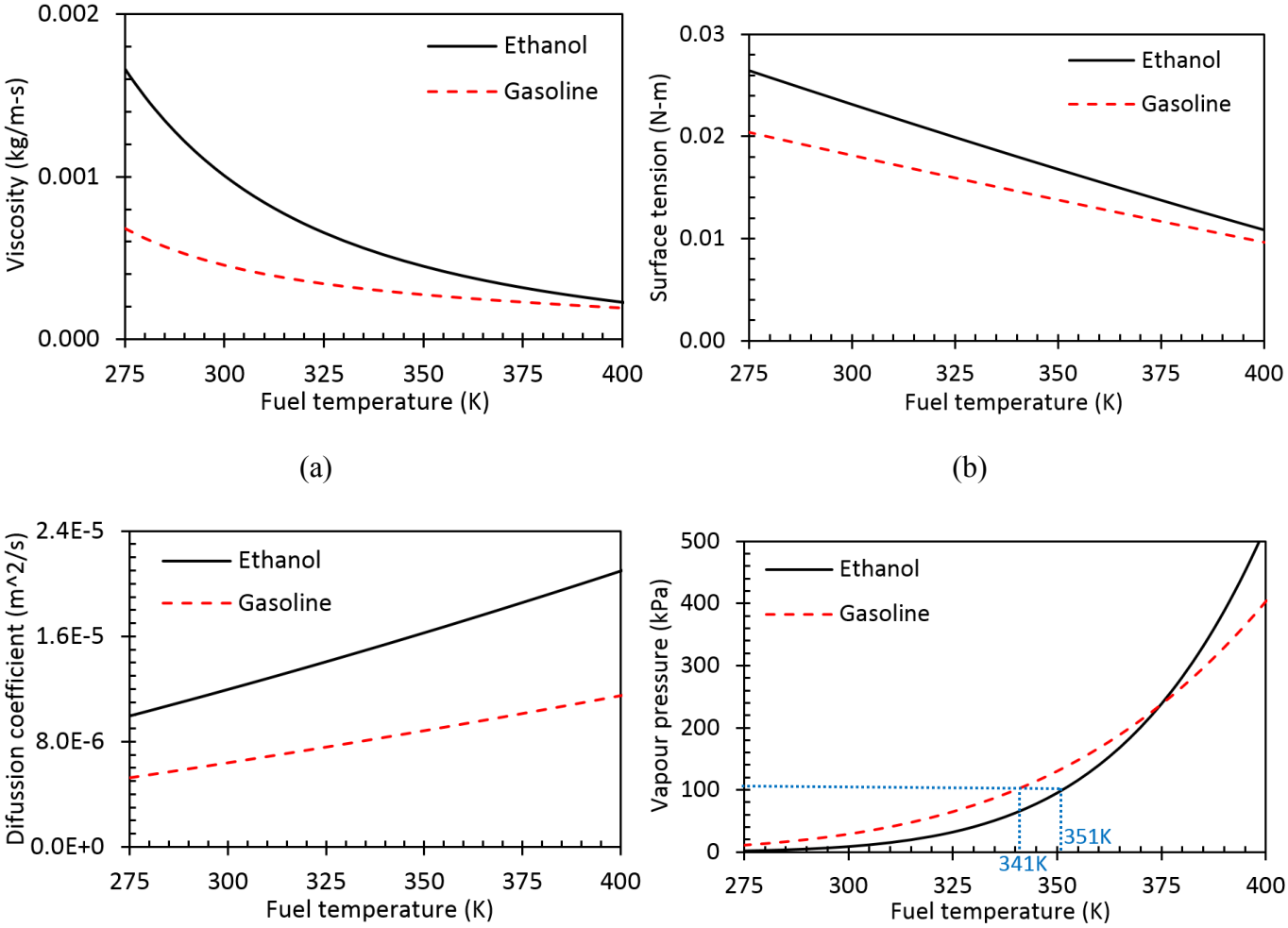

Fig. 2. Ethanol and gasoline fuel properties: (a) viscosity, (b) surface tension, (c) diffusion coefficient in air, and (d) saturation vapour pressure [34-36].

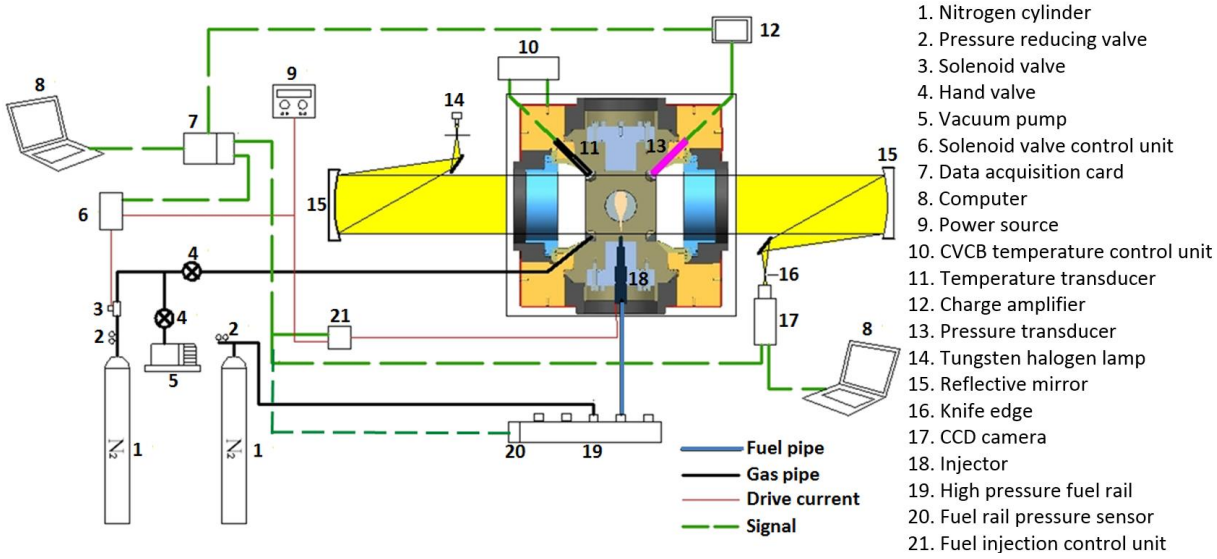

519

520 Fig. 3. Schematic diagram of the experimental apparatus.

521

522

523

524

525

526

527

528

529

530

531

532

533

534

535

(a) background image (b) raw spray image (c) background corrected

(d) binary image (e) detected spray boundary (f) processed spray image

Fig. 4. Shadowgraphy spray image processing method.

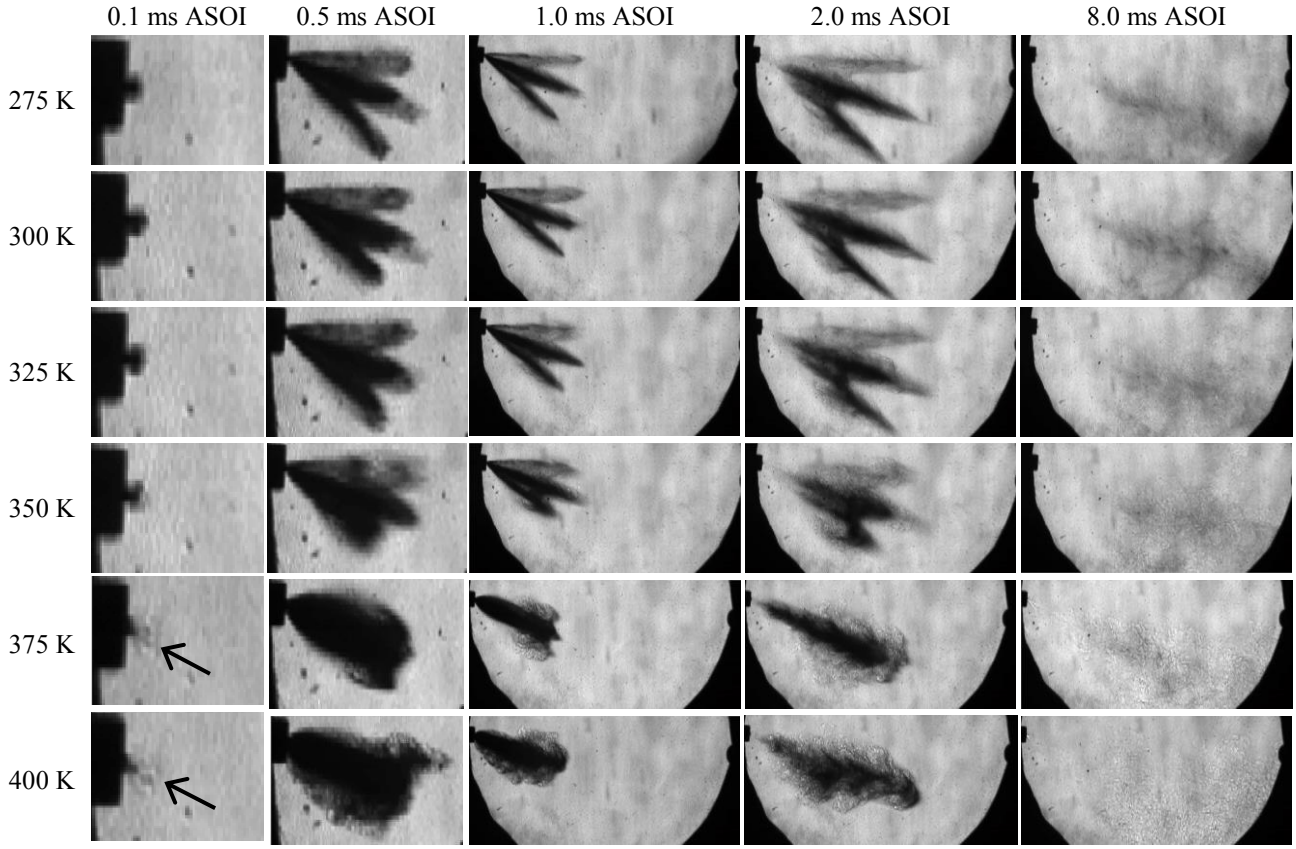

559 Fig. 5. Ethanol spray images in non-evaporating, normal-evaporating and flash-boiling conditions. (Please refer
560 to the electronic version of Fig. 5 for a clearer interpretation of the droplet explosion.)

561

562

563

564

565

566

567

568

569

570

571

572

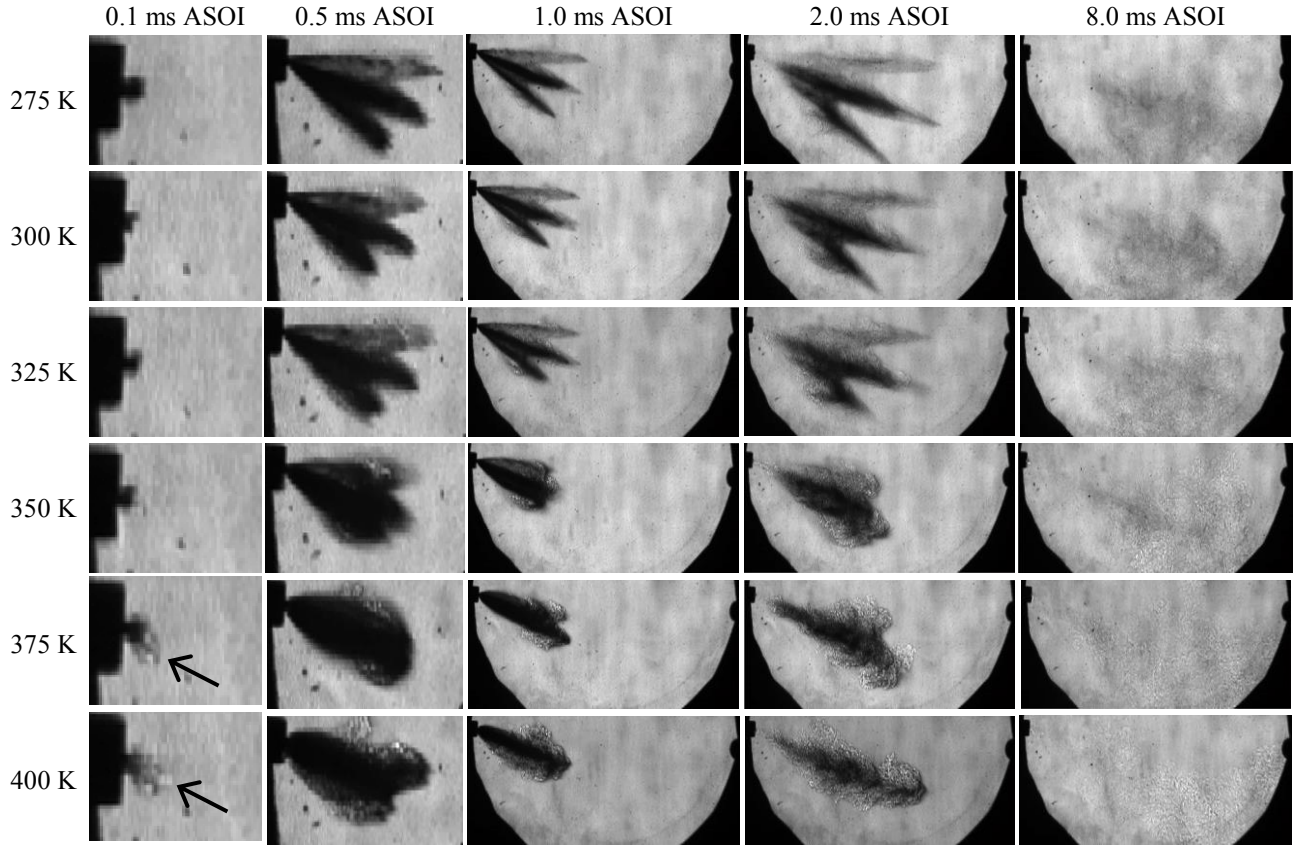

Fig. 6. Gasoline spray images in non-evaporating, normal-evaporating and flash-boiling conditions. (Please refer to the electronic version of Fig. 6 for a clearer interpretation of the droplet explosion.)

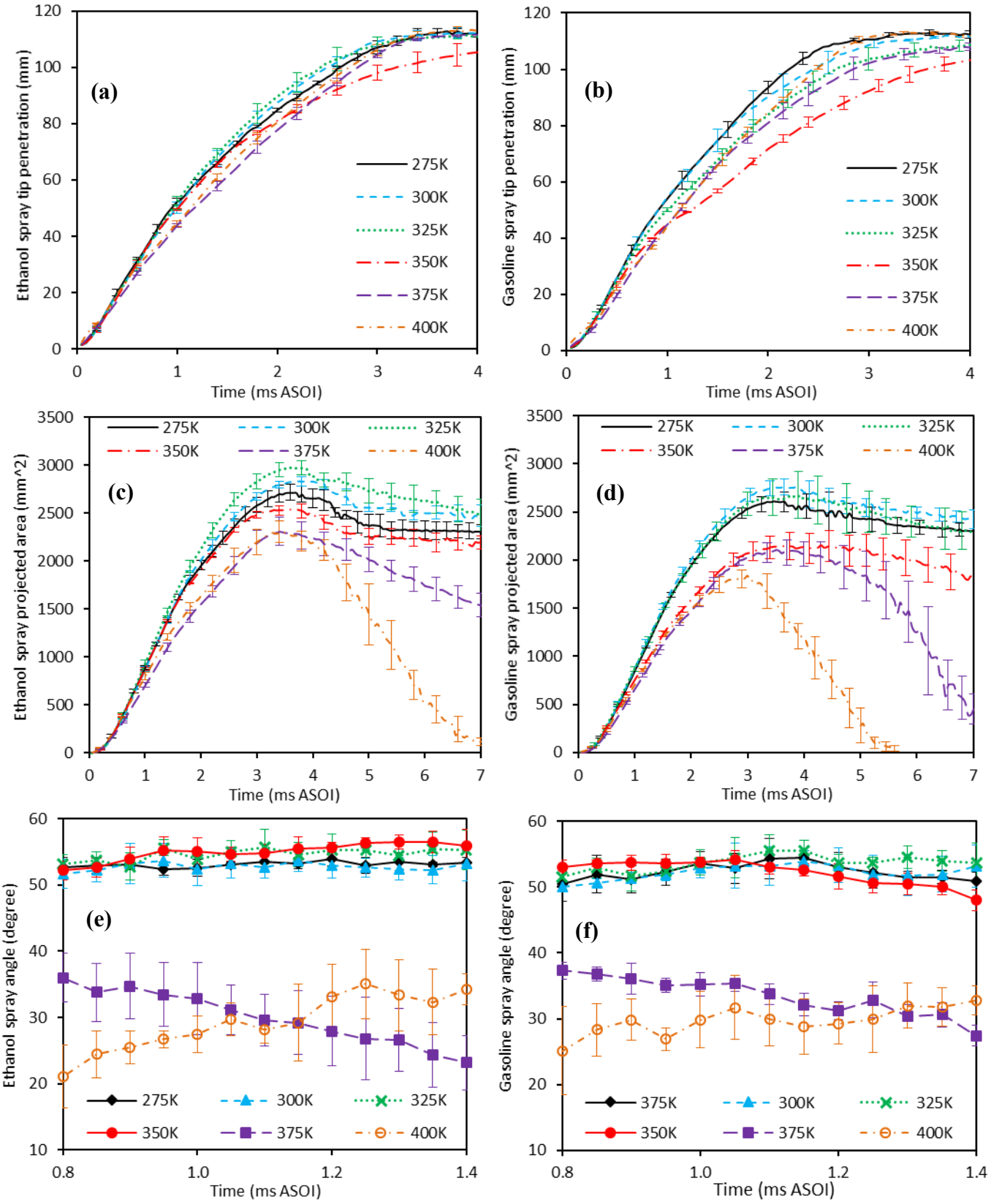

Fig. 7. Macroscopic spray characteristics: (a) ethanol spray tip penetration, (b) gasoline spray tip penetration, (c) ethanol spray projected area, (d) gasoline spray projected area, (e) ethanol spray angle, (f) gasoline spray angle.

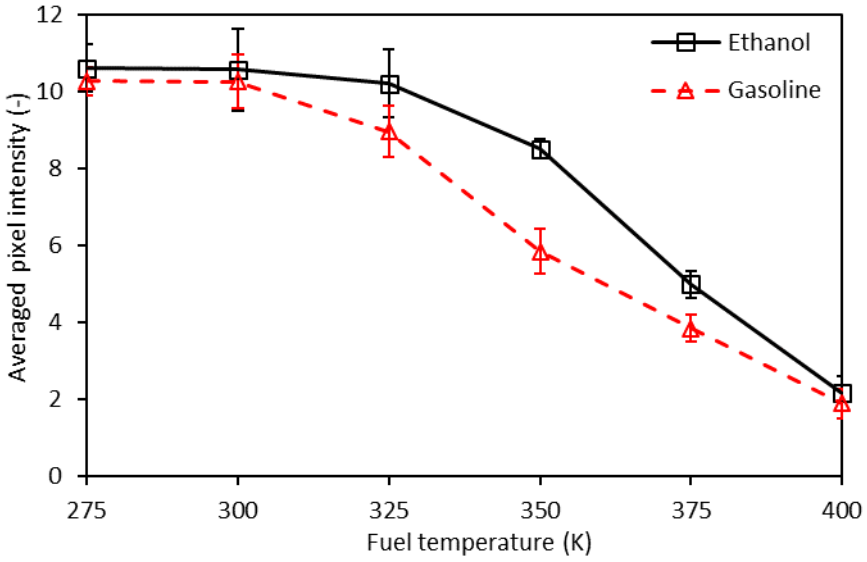

Fig. 8. Pixel intensity at 8.0 ms ASOI in non-evaporating, normal-evaporating and flash-boiling conditions.

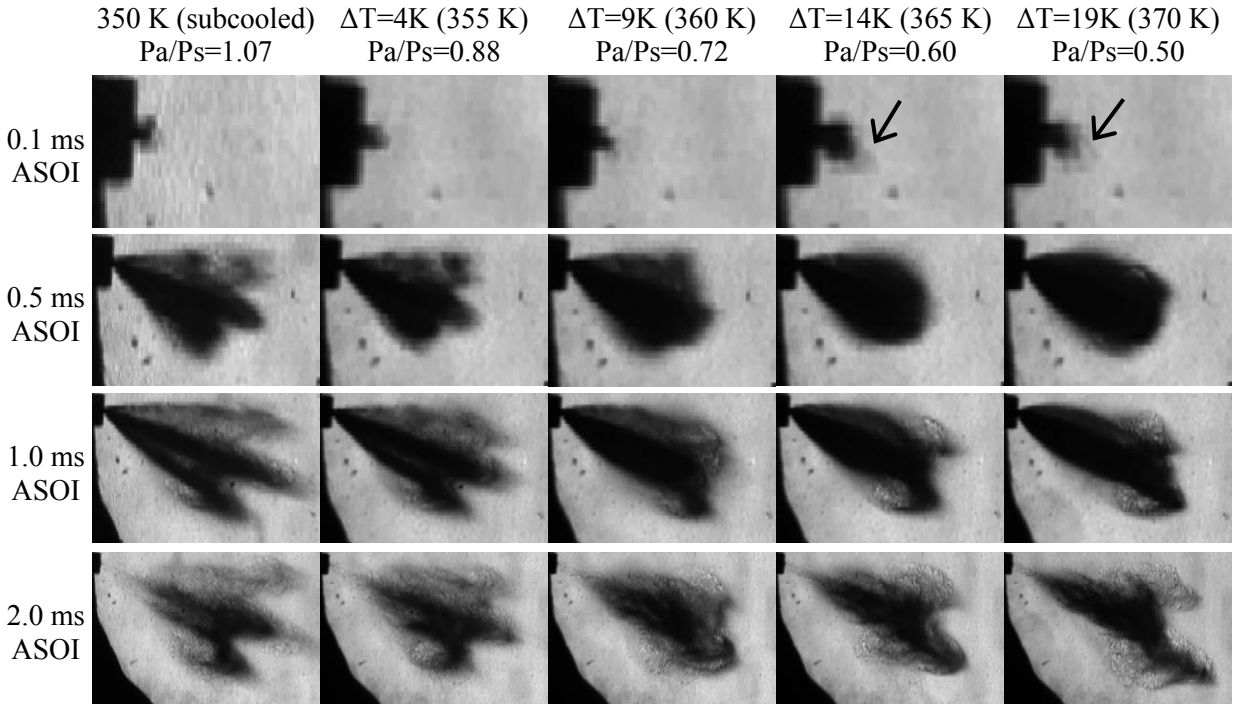

610 (a)

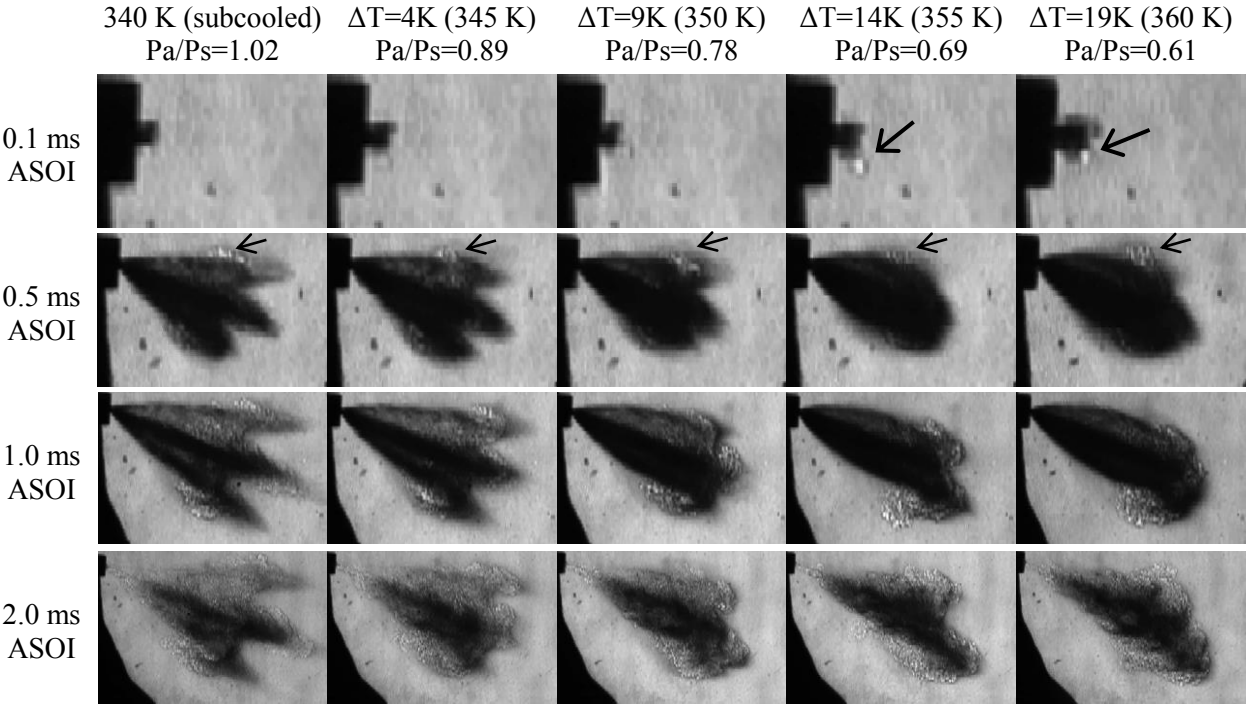

611 (b)

612 Fig. 9. Ethanol (a) and gasoline (b) spray images in the transition process. (Please refer to the electronic version

613 of Fig. 9 for a clearer interpretation of the spray cloud.)

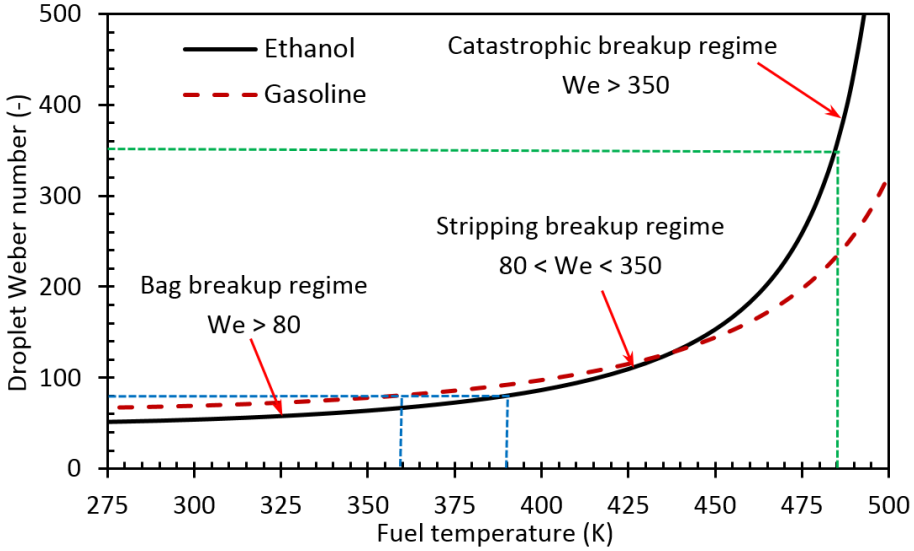

Fig. 10. Weber numbers of primary break-up droplets of ethanol and gasoline sprays at the nozzle exit with different fuel temperatures. The velocity of the primary droplet is assumed be the jet velocity [33, 50]. The diameter is determined based on the blob injection concept [51-53].

632 Table 1. Saturation vapour pressures of ethanol and gasoline fuels at the temperatures investigated [34-36]

Fuel temperature (K)	275	300	325	350	375	400
Ethanol vapour pressure (kPa)	1.83	8.77	32.09	95.07	238.42	523.05
Gasoline vapour pressure (kPa)	11.05	28.83	64.90	130.11	237.75	402.90

633